Oxidation of Chloride Ion on Platinum Electrode: Dynamics of Electrode Passivation and its Effect on Oxidation Kinetics

ARTICLE *in* INDUSTRIAL & ENGINEERING CHEMISTRY RESEARCH · AUGUST 2011

Impact Factor: 2.59 · DOI: 10.1021/ie200663a

3 AUTHORS:

Rajkumar Patil
Indian Institute of Technology Bombay
7 PUBLICATIONS **12** CITATIONS
SEE PROFILE

Vinay Juvekar
Indian Institute of Technology Bombay
78 PUBLICATIONS **732** CITATIONS
SEE PROFILE

Vijay M. Naik
Indian Institute of Technology Bombay
12 PUBLICATIONS **36** CITATIONS
SEE PROFILE

I&EC research
Industrial & Engineering Chemistry Research

ARTICLE

pubs.acs.org/IECR

Oxidation of Chloride Ion on Platinum Electrode: Dynamics of Electrode Passivation and its Effect on Oxidation Kinetics

Rajkumar S. Patil, Vinay A. Juvekar,* and Vijay M. Naik

Department of Chemical Engineering, Indian Institute of Technology Bombay, Powai, Mumbai-400076, India

ABSTRACT: Kinetics of oxidation of chloride ion is studied on both active platinum electrode and that undergoing transient passivation. Experiments are conducted in concentrated NaCl solution at rotating disk electrode. It is observed that on the active platinum electrode, oxidation is very fast, and hence the current density is controlled by the ohmic resistance of the solution. Electrode kinetics becomes important only when the electrode is passivated to a significant extent. Kinetics of chloride oxidation on the electrode undergoing passivation is modeled using the Butler−Volmer equation, in which the contribution from the ohmic resistance of the solution is incorporated. Two regimes of passivation are identified. The first is the fast regime corresponding to the formation of the platinum oxide monolayer. In this regime, the rate of passivation is first order in the concentration of the metal sites on the surface. In the slow passivation regime, the exchange current density for chloride oxidation is found to vary inversely with square root of time. This regime is modeled by considering unsteady diffusion of oxygen ions through the metal lattice. From this analysis it is concluded that the chloride oxidation current is almost totally contributed by a small fraction of the active metal sites which are continuously being regenerated as a result of diffusion of oxygen ions from the surface into the bulk of the metal.

1. INTRODUCTION

Sodium hypochlorite is a powerful disinfectant, deodorizer, and bleaching agent. It can efficiently destroy disease-causing bacteria.[1] It is, therefore, widely used in households,[2] swimming pools,[3] hospitals[2] and also for treatment of effluents in textile industries.[4] In many situations, on-site production of hypochlorite, via electrochemical oxidation of sodium chloride, can be beneficial as compared to the chemical dosing of the active agent. In situ production avoids bulk storage and transport of hazardous as well as unstable sodium hypochlorite solution. Another important advantage of on-site production of hypochlorite is that it facilitates better control of the concentration of active agent in the water body.[5]

The industrially used anodic materials for the hypochlorite production are ruthenium and iridium oxide-coated titanium metal (dimensionally stable anode, DSA)[6−8] and doped diamond electrodes.[9] Kraft et al.[3,10] have studied hypochlorite production at very low concentrations of NaCl and found that iridium oxide coated titanium electrode is superior to platinum. The life of DSA is, however, short.[2,11] Use of platinum as anode is advantageous in this respect. Platinum, being a noble metal, is highly resistive to corrosive environment. Although more expensive for large scale industrial process, platinum electrode is likely to be more suitable for in situ production where in the required size of electrode is small and long life reliability is important.[2] However, one drawback of platinum electrode is that it undergoes passivation due to formation of oxide film. The exchange current density on the passive platinum electrode is substantially lower than that which can be achieved by dimensionally stable electrodes under identical conditions.

In the present study, we show that it is possible to sustain high activity of platinum electrode by periodically cycling it to sufficiently high cathodic overpotentials. We also show that the activity of such an electrode is so high that the rate of oxidation of chloride ion is determined solely by the ohmic resistance of the solution. Therefore, using the periodic cycling technique, it is possible to produce sodium hypochlorite at a very high rate using platinum electrode, thus rendering platinum as an ideal material for in situ production of hypochlorite.

The present study is therefore undertaken with the objective to study kinetics of electro-oxidation of chloride ions on the active platinum electrode as well as the electrode which is undergoing transient passivation. The result of these studies provides an insight into the mechanism of passivation of the platinum electrode.

The paper is presented as follows. First, the electrochemistry of the chloride ion oxidation along with the concomitant side reactions is discussed. Various mechanisms proposed in the literature for the passivation of platinum electrode at anodic potentials, both in the presence and in the absence of chloride ions, are then briefly discussed. Next we discuss cyclic voltammetry and chronoamperometry experiments in aqueous sodium chloride solution. The results and discussion is focused on elucidation of kinetics of chloride ion oxidation both on the active electrode and that undergoing passivation.

2. ELECTROCHEMISTRY OF CHLORIDE ION OXIDATION

The reaction of chloride ions at the electrode is described by the following equation

$$2Cl^- \leftrightarrow Cl_2 + 2e^- \quad E^0 = 1.359\ V \tag{1}$$

where E^0 is the standard electrode potential of the reaction.

Special Issue: Ananth Issue

Received: April 1, 2011
Accepted: July 19, 2011
Revised: July 17, 2011
Published: July 19, 2011

dx.doi.org/10.1021/ie200663a | *Ind. Eng. Chem. Res.* 2011, 50, 12946–12959

The Nernst potential for the reaction can be estimated using the following equation

$$E = E^0 - \frac{RT}{2F} \ln\left(\frac{a_{Cl^-}{}^2}{p_{Cl_2}}\right) \quad (2)$$

Kinetics of chloride ion oxidation on platinum electrode has been well studied. The proposed mechanism views the reaction to be occurring in two steps. The first is the formation of metal-chloride bond with removal of electron. ($Cl^- + Pt \leftrightarrow PtCl + e^-$). This step is followed by reaction of the metal-chloride bond with chloride ion in the solution, which results in regeneration of the metal ($Cl^- + PtCl \leftrightarrow Pt + Cl_2$). Frumkin and Tedoradze[12] have postulated that the rate controlling step is the formation of metal-chloride bond (the first step of the sequence). Tedoradze[13] and Chang and Wick[14] have also shown that the rate determining step is the electrochemical step involving one electron transfer (i.e., $Cl^- \leftrightarrow Cl + e^-$). Thomassen et al.[15] however differ from the previous works. They studied the reverse reaction, i.e. chlorine reduction on electrochemically oxidized platinum and found that the rate controlling step is chemical adsorption of chlorine (i.e., $Pt + Cl_2 \leftrightarrow Cl^- + PtCl$). Tilak[16] has postulated that the rate controlling step in chloride oxidation is the recombination of metal-chloride species to form metal and chlorine ($PtCl + PtCl \leftrightarrow 2Pt + Cl_2$). Similar conclusion is also arrived at by Conway and Novak.[17] Dickinson et al.[18] have postulated that both the metal chloride bonding and reaction of bonded (or adsorbed) chlorine with chloride ions have comparable rate. Burrows et al.[19] have shown that on an active platinum surface, the postulate of Frumkin and Tedoradze[12] is correct.

The major anodic side reaction is oxidation of water.

$$2H_2O \leftrightarrow O_2 + 4H^+ + 4e^- \quad E^0 = 1.229\ V \quad (3)$$

It has been observed that formation of oxide film is necessary for evolution of oxygen on platinum surface.[20−25] Hence most studies on oxygen evolution reaction have been conducted using anodized platinum electrode. Mechanism of the reaction both in acidic and alkaline media has been investigated by several investigators.[21,26−30] Damjanovic et al.[31] have systematically studied the oxygen evolution reaction in perchloric acid. They have listed fourteen distinct mechanisms for the oxygen evolution reaction, some of which are proposed by them and some are from the previous literature. They have tried to distinguish various mechanisms on the basis of the Tafel slope, and the effect of pH and partial pressure of oxygen on the current density. Based on the Tafel slope, they concluded that the rate controlling step is the primary water discharge step which can be written as $Pt + H_2O \rightarrow PtOH + H^+ + e^-$. The rate of the reaction is therefore expected to depend on the concentration of water on the surface of the electrode. In the presence of NaCl, chloride ions compete with water molecules to occupy the electrode surface. At the highly positive potentials required for oxygen evolution reaction, the concentration of the chloride ions on the electrode surface is expected to be very high because of their negative charge. There is also a strong tendency of halide ions to be specifically adsorbed on platinum as demonstrated by several workers.[32−42] Using impedance spectroscopy, Breiter[43] has estimated the effect of halide ions on the capacitance of the double layer on platinum electrode and shown that nearly monolayer coverage of chloride ions on platinum electrode is attained at as low bulk concentration as 0.01 M. Since in the present work, most of the experiments have been performed using NaCl concentrations, which are greater than 0.25M, we can assume water adsorption on the electrode to be negligibly small. Specific adsorption of chloride ions begin right from the hydrogen evolution region. Equilibrium coverage of chloride ions is found to vary linearly with potential.[44,45] Li et al.[46] studied surface coverage of chloride ion using QCM and found that the surface coverage of chloride is 100% between −0.5 and 0.6 V.

Based on these findings, we conclude that in the presence of high concentration of chloride ions, the contribution to the total current by oxygen evolution reaction can be neglected.

Chlorine formed by reaction 1 reacts further with water to form hypochlorite ions according to the eq 4 and 5[47]

$$Cl_2 + H_2O \leftrightarrow HOCl + Cl^- + H^+ \quad K = 1.04 \times 10^{-3}\ M^2 \quad (4)$$

$$HOCl \leftrightarrow H^+ + OCl^- \quad pK_a = 7.5 \quad (5)$$

These reactions are extremely fast and can be treated as equilibrium steps. Hence the overall rate of hypochlorite ion formation is controlled by the electrochemical reaction 1.

In an electrolytic cell producing hypochlorite ion, the auxiliary reaction at the cathode is hydrogen production.

$$2H_2O + 2e^- \leftrightarrow H_2 + 2OH^- \quad E^0 = -0.7828\ V \quad (6)$$

The hydroxyl ions generated at the cathode neutralize the protons generated at the anode by reactions 4 and 5. Thus the pH of the solution remains nearly constant.

Hypochlorite ions undergo further oxidation to chlorate ions[48]

$$6ClO^- + 3H_2O \leftrightarrow 2ClO_3^- + 6H^+ + 4Cl^- + \frac{3}{2}O_2 + 6e^- \quad (7)$$

This reaction is slow and becomes important only at high concentrations of the hypochlorite ions.

3. PASSIVATION OF PLATINUM ELECTRODE

When platinum is used as anode in aqueous solutions, it undergoes passivation because of formation of oxide film, by reaction with water. Oxide film can both be formed[49−52] and reduced[49,50,53,54] electrochemically. Gillman[55] has proposed the following mechanism for passivation, which postulates formation of different oxides of platinum. At potentials lower than 1 V, the following reactions occur, leading to formation of platinum hydroxide and monoxide.

$$Pt + H_2O \leftrightarrow Pt - OH + H^+ + e^-$$
$$Pt - OH \leftrightarrow PtO + H^+ + e^- \quad (8)$$

At potentials above 1.2 V, platinum monoxide oxidizes further to dioxide.

$$PtO + H_2O \leftrightarrow PtO_2 + 2H^+ + e^- \quad (9)$$

Numerous studies have been performed on the nature and growth of the oxide film in the absence of chloride ions.[15−27] Biegler and Woods[56] observed the limiting surface coverage of oxygen as 2.66 atoms per atom of platinum. They also found linear dependence of the coverage on the potential below the limiting coverage.

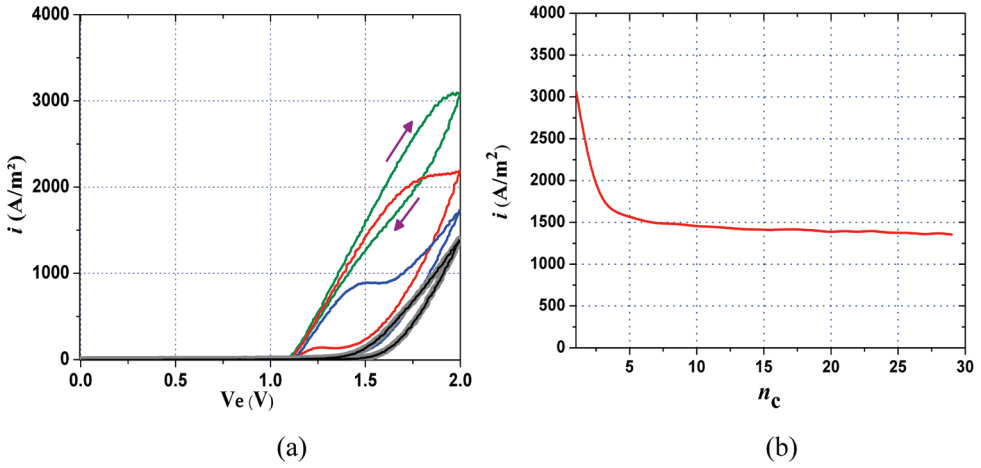

Figure 1. Sequence of cyclic voltammograms on platinum rotating disk electrode in the potential range from 0 to 2 V (reference electrode: saturated calomel). The electrode was preactivated just before conducting the experiment. Parameters: Concentration of NaCl, 1 M; speed of rotation of disk, 50 Hz; scan rate, 300 mV·s^{-1}; number of cycles. 30. (For clarity, only the first three and the last two cycles are displayed in Figure 1a.) In Figure 1b, anodic peak current density at 2 V (obtained from Figure 1a) is plotted against cycle number n_c. Line colors in Figure 1a: green, cycle 1; red, cycle 2; blue, cycle 3; gray, cycle 29; black, cycle 30.

The issue of whether the oxygen exists on platinum surface as a chemisorbed species or in the form of oxides is still not completely resolved. Feldberg et al.[57] have postulated that oxide film is chemisorbed oxygen rather than the oxides of platinum. Some other workers[51,58,59] have reasoned that the surface oxidation involves formation of $^{\bullet}$OOH radical, which is reduced to hydroxide as the first step and then to oxide as the second step.

The rate of growth of the oxide film is an indicator of the passivation mechanism and hence has been well studied and modeled. Goswamy and Staehle[60] reported logarithmic growth of the oxide film with time. Several models have been proposed to explain this time dependence of growth. In the Mott and Cabrera model,[61] metal cations are assumed to be transported across the oxide film to the interface. This transport is assisted by the field that exists in the film. In the Sato and Cohen model,[62] the layer of oxygen, which is adsorbed on the surface, exchanges places with the underlying metal atoms. Another layer of oxygen is adsorbed and the process continues. This mechanism is known as the place exchange mechanism. Sato and Notoya[63] modified the Sato-Cohen model by including the effect of electrode potential on migration of oxygen ions and obtained the logarithmic growth law. Fehlner and Mott[64] modified Mott-Cabrera model by incorporating diffusion and migration of oxygen anion through the film. They assumed that the field strength in the film, which assists the migration of oxygen ions, is independent of its thickness. They also postulated that the rate limiting step is slow oxidation of the metal at the metal-solution interface and its activation energy increases linearly with the film thickness. There are certain reservations about the Mott−Cabrera model. Several workers have observed that surface oxidation (Reaction 8) is a very rapid step and cannot possibly be rate controlling. Also the logarithmic growth law is not found to be universally valid. Chao et al.[65] have proposed a more general model called "point defect model" to explain these anomalies. Since, in general, the oxide films have very low conductivity, very high field is generated inside the films. The magnitude of this field approaches the threshold for dielectric breakdown (10^8 V·m^{-1}). At high fields, the film behaves as a semiconductor. Also, point defects exist in the metal as well as in the oxide film. These defects can either transport holes (positive charges) or electrons. The overall rate is governed by the transport of electrons and holes through the film or their transfer across the metal-solution or metal film interface. Their model predicts logarithmic growth rate only for thick films. Also, according to this model, the transient current during the passivation process varies inversely with time for thick films, but inversely with square root time for thin films.

It is important to note that the aforementioned models are appropriate only for the oxide films having very low conductivity, that is, iron oxide. The oxide film of platinum does not belong to this category. Shibata[66] anodized platinum in 0.5 M sulfuric acid and measured resistance of the oxide film formed. He observed formation of two types of films. The initially formed film is a monolayer and has conductivity equal to that of the metal. The multilayer film, which forms later consists of PtO_2 and has conductivity in the range of 0.1 to 0.2 S·m^{-1}. Although this conductivity is much less that of metal, it is still several orders of magnitude higher than that of iron oxide. Hence the electric field which exists in the platinum oxide film is expected to be much smaller than the breakdown threshold. The validity of the point defect model is therefore questionable in the case of platinum.

Passivation of platinum electrode in aqueous NaCl is also well studied.[67,68] It is also attributed to formation of the oxide film.[68,69] However, the chloride ions retard the film formation.[43] Obrucheva[70] observed that when HCl was added to sulfuric acid, the extent of anodization was significantly reduced at the same anodic potential. The inhibition is attributed to competition between specifically adsorbed chloride ions and oxygen.[34,70−72]

Kuhn and Wright[73] have shown that in the presence of NaCl the film grows in two stages with increasing potential. First stage is the formation of PtO. This occurs at lower potentials. The second involves formation of PtO_2. This occurs at higher potential. The transition potential increases with concentration of NaCl and temperature.

4. EXPERIMENTAL SECTION

All experiments were conducted on a platinum rotating disk electrode (platinum disk embedded in a Teflon sleeve) having radius of 2.5 mm. The speed of rotation of the electrode was

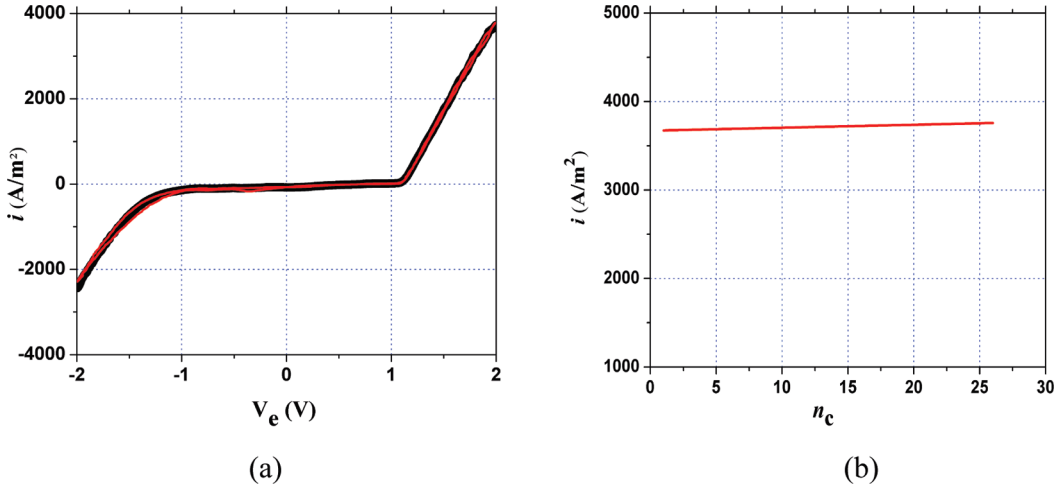

Figure 2. Sequence of cyclic voltammograms on platinum rotating disk electrode in the potential range −2 to 2 V (reference electrode: saturated calomel). The electrode was preactivated just before conducting the experiment. Parameters: concentration of NaCl, 1 M; speed of rotation of disk, 50 Hz; scan rate, 500 mV·s^{-1}; number of cycles 26. (For clarity, only the first and the last cycle are displayed in Figure 2a.) In Figure 2b, anodic peak current density at 2 V (obtained from Figure 2a) is plotted against cycle number n_c. Line colors in Figure 2a: black, cycle 1; red, cycle 26.

50 Hz in all experiments, except those where the effect of the speed of rotation was studied. A single compartment, three electrodes system is used, where the counterelectrode was platinum plate having 1 cm^2 area, and the reference electrode was saturated calomel electrode (SCE). A Luggin capillary was attached to the reference electrode. The tip of the capillary was placed close to the disk. The volume of the solution used for electrolysis was about 100 mL. Experiments were conducted using an electrochemical workstation (Model: CHI6089D, CH instruments, USA). The workstation has potential range of ±10 V, current range of ±250 mA, and the input impedance of reference electrode of 10^{12} Ω. Temperature was 298 K in all experiments. No attempt was made to control the pH of the solution. However, pH of the solution was found to remain within the range of 6.5 to 7.0 in all experiments.

Sodium chloride used was analytical grade (Merck, India), Milli-Q water was used for preparing the solutions. Conductivity of the sodium chloride solutions was measured using Thermo Orion conductivity meter. The probes having appropriate cell constants were used in different ranges of sodium chloride concentrations. These cells were precalibrated using the standard solutions supplied by the company. The accuracy of the meter was also tested by comparing the conductivity values, measured by the meter, with those reported in the literature.[74] The difference between two sets of the values was within 3%.

Three kinds of experiments were performed, namely, cyclic voltammetry, chronoamperometry, and reverse linear sweep voltammetry. Before conducting the actual experiment, the electrode was preactivated by cycling between −2.0 V and 2.0 V for 10 cycles, at the sweep rate of 500 mV·s^{-1}.

5. RESULTS AND DISCUSSION

5.1. Sequence of Cyclic Voltammograms on Platinum Electrode. Figure 1a displays a sequence of cyclic voltammograms performed at the rotating disk electrode in 1 M NaCl solution. The potential range is 0−2 V with reference to saturated calomel electrode, the scan rate is 300 mV·s^{-1}, and the disk speed is 50 Hz.

A total of thirty cycles were performed. However, for the sake of clarity, the voltammograms of only the first three and the last two cycles have been displayed in Figure 1a. On the basis of the previous studies[43] it may be seen from the Figure 1a that significant anodic current is observed only when the electrode potential is above 1.1 V, which is the equilibrium potential for oxidation of chloride ions (eq 1). During the forward sweep of the first cycle, current density varies linearly with potential, but levels off when the potential approaches 2 V. Moreover, current density during the reverse sweep is substantially lower than that during the forward sweep. These observations are indicative of passivation of the electrode during the forward and a part of the reverse sweep. Although, certain degree of reactivation can possibly occur during the reverse sweep, electrode is not fully restored at the end of the first cycle. This is evident from the fact that the current density during the subsequent cycles is lower than that during the first cycle. The rate of passivation is faster during the initial cycles, but slows down, and finally the voltammograms of the last two cycles (29th and 30th) overlap each other as seen in Figure 1a. However, note that the hysteresis still persists, indicating that passivation continuous even at this stage. However, reactivation during the reverse sweep almost fully restores the electrode to the state at the beginning of the previous cycle. Thus cyclical steady state is reached after about 30 cycles.

A clearer idea about passivation is obtained from Figure 1b, which plots current density at the electrode potential of 2 V, versus cycle number. It is seen that the current decreases sharply during the first few cycles but slowly after about 15 cycles. It is important to note that fall in the peak current is a measure of the extent of net passivation of the electrode which is the balance of the passivation and the partial reactivation processes.

To test whether it is possible to completely reactivate the electrode by sweeping it to a sufficiently high cathodic potential (say −2.0 V), cyclic voltammetry was performed in the potential range of −2 to 2 V. Again a series of 26 cycles were performed and the resulting voltammograms are presented in Figure 2a and b.

Figure 2a clearly shows that the voltammograms of the first and the twenty-sixth cycles almost coincide with each other. The peak currents are also almost identical in all cycles, indicating that the electrode is restored at the end of each cycle to its initial state.

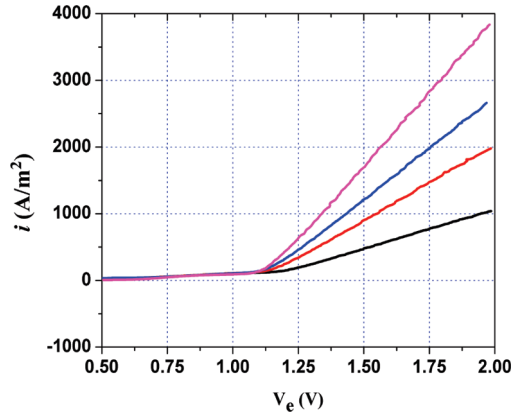

Figure 3. Anodic portions of the voltammograms on rotating disk electrode in different concentrations of NaCl solution. The electrode was preactivated just before conducting the experiment. Parameters: speed of rotation of disk, 50 Hz; scan rate, 5000 mV·s^{-1}; potential range, −2.0 V to 2.0 V. Line colors: black, 0.25 M; red, 0.5 M; blue, 0.75 M; magenta, 1.0 M. (Small anodic current seen in the region between 0.5 V to 1.1 V is probably due to oxidation of adsorbed hydrogen gas on platinum electrode.)

Also almost no hysteresis is present in the voltammograms, implying that electrode retains its initial high activity throughout the potential sweep. In fact, in Figure 2b, which plots the current density at 2 V, as a function of number of cycles, shows a slight, but perceptible improvement in the activity with cycling.

5.2. Kinetics of Chloride Ion Oxidation on Active Platinum Electrode. Another important observation from Figure 2a is that the anodic current density varies linearly with overpotential. The slope of this plot represents the specific resistance of the system to the transfer of current across the electrodes ($d\eta/di$). If charge transfer were controlling, the resistance would have decreased with increasing in the overpotential as predicted by the Butler−Volmer equation. The only resistance, which is independent of the overpotential, is the ohmic resistance of the solution. For the rotating disk electrode, Newman[75] has derived the following expression for the ohmic resistance R_S for a disk electrode placed in an infinite solution.

$$R_s = \frac{1}{A_e}\frac{d\eta}{di} = \frac{1}{4r_d\kappa_e} \tag{11}$$

where η is the overpotential A_e represents the electrode area ($= \pi r_d^2$), r_d being the radius of the disk and κ_e is the conductivity of the solution. This expression can be used to estimate the conductivity of the solution as follows. The slope of the straight line portion of the plot in Figure 2a is $s = di/dV_e = di/d\eta$. Using this expression in eq 11, we get

$$\kappa_e = \frac{\pi r_d s}{4} \tag{12}$$

If the ohmic resistance is controlling the current, then the solution conductivity, estimated using eq 12, should match with the actual conductivity. To verify this, cyclic voltammetry was conducted using four different concentrations of NaCl solution in the range of 0.25 to 1 M. Potential range used was −2 to2 V and the sweep rate was 5000 mV·s^{-1}. The anodic portions of the resulting voltammograms are shown in Figure 3.

The conductivities of the solutions were estimated from the slopes of the straight lines using eq 12. The conductivities of these solutions were also measured using conductivity meter.

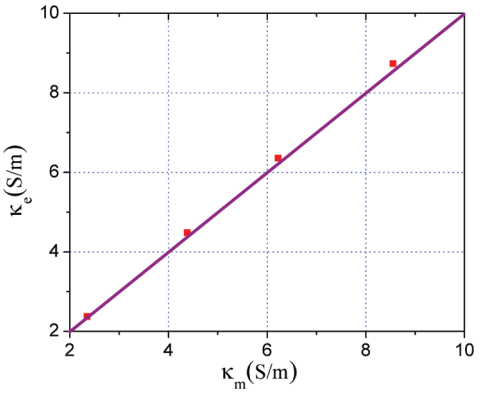

Figure 4. Parity plot for conductivity estimated from Figure 3 (κ_e) and measured using conductivity meter (κ_m).

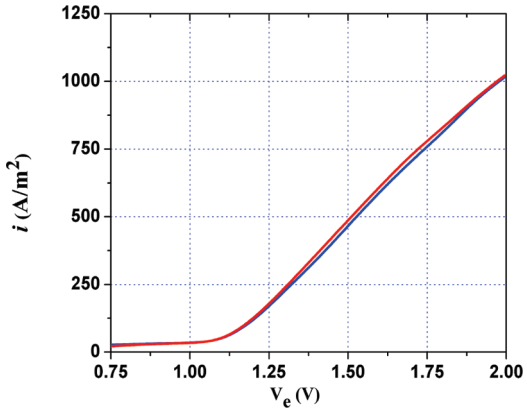

Figure 5. Effect of speed of rotation of platinum disk on anodic current density. The electrode was preactivated just before conducting the experiment. Parameters: concentration of NaCl, 0.25 M; scan rate, 1000 mV·s^{-1}; potential range, −2.0 to 2.0 V. (For better clarity, voltammograms are plotted in the range of 0.75−2.0 V.) Line colors: blue, 8 Hz; red, 80 Hz.

The comparison between the two sets of values of conductivity is made in Figure 4 in the form of a parity plot.

A good parity in Figure 4 implies that the ohmic resistance of the solution is indeed the controlling resistance. Transfer of the chloride ions to the electrode occurs by conduction and diffusion. To check whether or not the contribution due to diffusion is important, cyclic voltammetry experiments were performed in 0.25 M NaCl solution over the disk-speed range of 8 to 80 Hz, and the potential range of −2.0 V to 2.0 V. The anodic portions of the voltammograms differ insignificantly as shown in Figure 5. If the diffusion contribution were important, the current density would increased significantly with increase in speed of the rotating disk. The absence of this dependence in Figure 5 is an indication that the diffusion contribution to the total current is negligible.

5.3. Passivation Characteristics of Platinum Electrode. Effect of the scan rate on the rate of passivation of electrode is illustrated in Figure 6.

In this experiment, electrode was swept between −2.0 and 4.0 V at different scan rates in the range of 10 mV·s^{-1} to 2500 mV·s^{-1}. We show parts of the voltammograms in the anodic region.

All voltammograms follow a single manifold, which corresponds to ohmic regime, up to a certain potential, and then

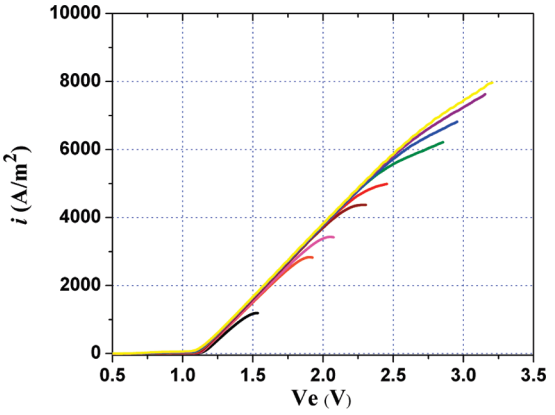

Figure 6. Effect of sweep rate on passivation of platinum rotating disk electrode. The electrode was preactivated just before conducting the experiment. Parameters: concentration of NaCl, 1 M; speed of rotation of disk, 50 Hz. Line color corresponds to scan rate: black, 10 $mV \cdot s^{-1}$; orange, 50 $mV \cdot s^{-1}$; magenta, 100 $mV \cdot s^{-1}$; brown, 250 $mV \cdot s^{-1}$; red, 500 $mV \cdot s^{-1}$; green, 1000 $mV \cdot s^{-1}$; blue, 1500 $mV \cdot s^{-1}$; purple, 2000 $mV \cdot s^{-1}$; yellow, 2500 $mV \cdot s^{-1}$.

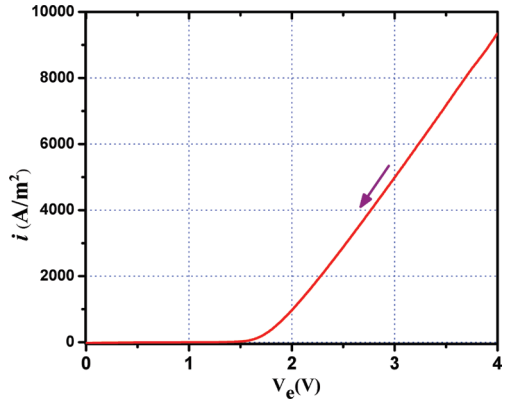

Figure 7. Reverse sweep voltammogram on a passive platinum electrode. After activation, the electrode is allowed to passivate at 2 V in 1 M NaCl for 400 s. Parameters: concentration of NaCl, 1 M; speed of rotation of disk, 50 Hz; scan rate, 1500 $mV \cdot s^{-1}$.

deviate from this manifold. Ohmic regime is a characteristic of the active electrode. The deviation from the manifold occurs due to passivation of the electrode. Higher the sweep rate, greater is the potential up to which the current density lies on the manifold. This trend is expected because passivation is a time dependent phenomenon. At higher sweep rate, the time required for the electrode to reach a given anodic potential is shorter, and therefore the electrode is passivated to a lesser extent during this time. Consequently, the electrode can scale a higher potential before it is sufficiently passivated so as to deviate from the ohmic manifold.

5.4. Ohmic Resistance of the Oxide Film on Platinum Electrode. If the oxide film is impervious, the reaction must occur on the oxide surface and the electrons should be conducted through the film to the metal. Since the resistance to transport of the current through the film is in series with the solution resistance, the total resistance would be the sum of the two resistances. To test whether or not the resistance of the oxide film is important, we conducted the following experiment.

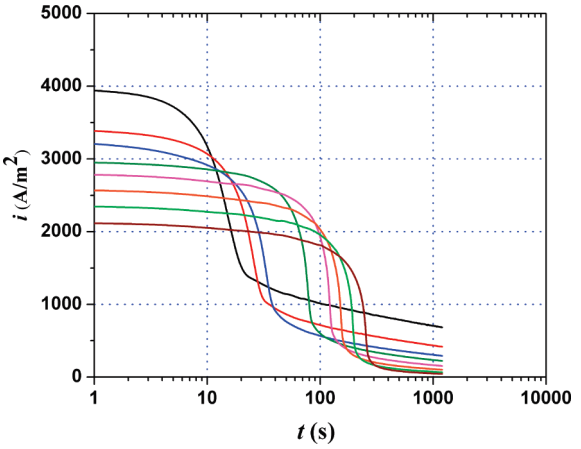

Figure 8. Chronoamperograms of platinum electrode undergoing passivation at different electrode potentials. In all experiments, the electrode was preactivated just before the experiment. Parameters: concentration of NaCl, 1 M; speed of rotation of disk, 50 Hz. Line color corresponds to electrode potential used for passivation: brown, 1.60; green, 1.65 V; orange, 1.7 V; pink, 1.75 V; dark green, 1.80 V; blue, 1.85 V; red, 1.90 V; black, 2.0 V.

Preactivated rotating disk electrode was passivated by maintaining it at 2 V in 1 M NaCl for 400 s. A reverse sweep voltammetry was then conducted between 4 and 0 V at the sweep rate of 1500 $mV \cdot s^{-1}$. The voltammogram during the reverse sweep step is shown in Figure 7. The slope of the straight line portion is, $s = 4.29 \times 10^3$ $(A \cdot m^{-2} \cdot V^{-1})$. From this slope, the apparent conductivity of the solution is estimated using eq 12 as 8.55 $(S \cdot m^{-1})$. This value agrees very well with the measured value of conductivity of 8.44 $(S \cdot m^{-1})$ of 1 M NaCl solution. This shows that even after the formation of the oxide film, the overall resistance is still controlled by the solution, indicating that the film of platinum oxide offers much lower ohmic resistance than the solution.

If we assume the thickness of the oxide film to be of the order of few angstroms and the conductivity of the film to be in the range of 0.11−0.21 $S \cdot m^{-1}$, based on the estimate of Shibata,[66] the resistance of the oxide film is estimated to be of the order of 10^{-5} ohm. This resistance is negligibly small compared to the resistance of the solution, which is about 10 ohm.

5.5. Kinetics of Chloride Ion Oxidation on Platinum Electrode Undergoing Passivation. Chronoamperometry, as well as reverse sweep voltammetry, were used to study the kinetics of chloride oxidation on a platinum electrode undergoing passivation. In the chronoamperometric experiments, the preactivated rotating disk electrode was held at a constant potential and the current was measured as a function of time. Experiments were conducted at different potentials in the range of 1.6−2 V. Figure 8 shows the chronoamperograms at different potentials. Three regimes are evident. Initially there is a current plateau. This is followed by the second regime where there is a rapid decrease in the current. In the third regime, we observe a slow decrease in current with time. During the first regime, the electrode is active and ohmic resistance controls the current. During the other two regimes, the electrode undergoes passivation, first at a faster rate and then at a slower rate.

In the reverse sweep voltammetry experiments, the preactivated electrode was allowed to passivate at 2 V potential for a specific period of time, and then its potential was swept back linearly in time to 0 V. The current was measured during the reverse sweep. The experiment was repeated for different durations of

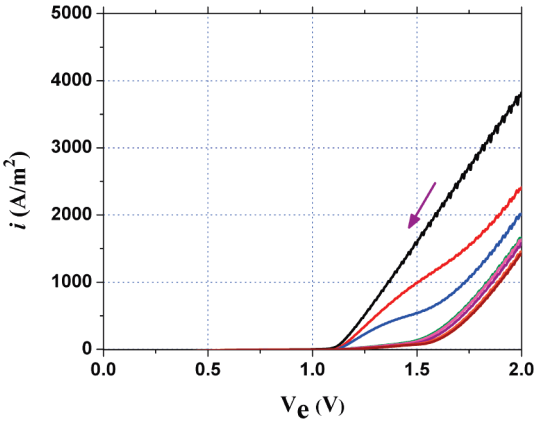

Figure 9. Reverse sweep voltammograms on platinum rotating disk electrode at different stages of passivation. In all experiments, electrode was preactivated before subjecting it to passivation. Parameters: concentration of NaCl, 1 M; speed of rotation of disk, 50 Hz; potential range, 2.0−0 V; scan rate, 1500 mV·s^{-1}. Line color corresponds to duration of passivation: black, 0 s; red, 5 s; blue, 6 s; green, 8.0 s; magenta, 8.5 s; purple, 9.0 s; orange, 12 s; brown, 13.5 s.

passivation. Figure 9 represents the linear reverse sweep voltammograms. The time duration of passivation are also listed in the Figure 9.

The voltammogram, on active electrode (passive time = 0) is a straight line right down to the equilibrium potential indicating that the ohmic resistance of the solution is controlling throughout the sweep. The intermediate voltammograms, where both the ohmic and the charge transfer resistances are important, have complex shapes. However, at longer passivation times, the voltammograms have familiar Butler−Volmer profiles.

5.6. Model for Kinetics of Electrooxidation of Chloride Ions. To explain the results presented in the previous sections, we model the kinetics of oxidation of chloride ion using the Butler−Volmer equation. The standard form of the Butler−Volmer equation is

$$i = i_0\left[\exp\left(\alpha\frac{F}{RT}\eta\right) - \exp\left(-(1-\alpha)\frac{F}{RT}\eta\right)\right] \tag{13}$$

The net available overpotential is the difference between the total available overpotential minus the ohmic drop in the solution around the working electrode. Thus

$$\eta = (V_e - V_{eq}) - iA_eR_s \tag{14}$$

where V_{eq} is the equilibrium electrode potential. R_S represents the ohmic resistance of the solution and is given by eq 11. A_e is the surface area of the electrode. Substituting this expression for η into eq 13, we get

$$i = i_0\left[\exp\left\{\alpha\frac{F}{RT}(V_e - V_{eq} - iA_eR_s)\right\} - \exp\left\{-(1-\alpha)\frac{F}{RT}(V_e - V_{eq} - iA_eR_s)\right\}\right] \tag{15}$$

At low overpotentials, we can linearize eq 15 and rearrange it to yield the following expression for the current density

$$i = \frac{i_0(F/RT)(V_e - V_{eq})}{1 + i_0(F/RT)A_eR_s} \tag{16}$$

If the electrode is not very active, i_0 is low so that $i_0(F/RT)A_eR_S \ll 1$. Equation 16 then reduces to $i = i_0(F/RT)(V_e - V_{eq})$, which is the familiar linear regime of the Butler−Volmer equation. However, when the electrode is very active, the magnitude of i_0 is sufficiently high to satisfy the condition $i_0(F/RT)A_eR_S \gg 1$. Equation 16 then reduces to

$$i = \frac{V_e - V_{eq}}{A_eR_s} \tag{17}$$

The current density, under this condition, is controlled by charge migration. Equation 17 indicates that the migration limiting current varies linearly with the electrode potential. The slope of the plot of straight line is $s = 1/A_eR_S$, and its intercept on the potential axis is V_{eq}. This interpretation is consistent with the experimental findings of Figure 3.

When the electrode undergoes passivation, i_0 decreases and beyond certain degree of passivation, the condition: $i_0(F/RT)A_eR_S \gg 1$ is no more valid. Equation 17 does not hold good, but eq 16 can still be used to compute the current density. With further passivation, the exchange current density is low enough so that the condition $i_0(F/RT)A_eR_S$ becomes much less than unity. In such cases, we can neglect the ohmic resistance in the Butler−Volmer equation at low overpotentials and write it in the conventional form. However, at sufficiently high potentials, system again transits to the migration control regime. To see how, we differentiate the Tafel form of eq 15 with respect to electrode potential

$$\frac{di}{dV_e} = i_0\exp\left\{\alpha\frac{F}{RT}(V_e - V_{eq} - iA_eR_s)\right\}\alpha\frac{F}{RT}\left(1 - \frac{di}{dV_e}A_eR_s\right) \tag{18}$$

Equation 18 can be solved for di/dV_e to yield

$$\frac{di}{dV_e} = \frac{\alpha\frac{F}{RT}i}{1 + A_eR_s\alpha\frac{F}{RT}i} \tag{19}$$

when $i\alpha(F/RT)A_eR_S \gg 1$ eq 19 simplifies to

$$\frac{di}{dV_e} = \frac{1}{A_eR_s} \tag{20}$$

The plot of current density versus potential is again a straight line with the slope $s = 1/A_eR_S$. However, in contrast to eq 16, the intercept of the straight line on the potential axis is greater than V_{eq}. This is clearly demonstrated in Figure 7, which is the reverse sweep voltammogram on a passive electrode. The plot is a straight line after the current density of about 1000 A·m^{-2}. The intercept of this straight line on the potential axis is about 1.7 V, which substantially greater than V_{eq} (1.1 V) . The value of $i\alpha(F/RT)A_eR_S$, for i = 1000 A·m^{-2}, is approximately 4.5, which can be considered large enough so that eq 20 is obeyed.

The important point to note is that, if the diffusion limitation is not present in the system, the migration regime is inevitably attained at sufficiently high electrode potentials for any electrochemical reaction that is governed by the Butler−Volmer equation. The reason this regime is not observed in the experiments, which are designed to study electrode kinetics, is that in those experiments, high concentration of the supporting electrolyte is used, in conjunction with low concentration of the reacting species. The diffusion limiting current is therefore reached well before the migration controlled regime sets in. The reason why the diffusion limiting current is not important in the present case is that a single species (i.e., NaCl), which is present in high

Table 1. Ohmic Resistance of the Solution around a Disk Electrode[a]

z/r_d	0.1	0.2	0.5	10
R_s/R_{max}	0.126	0.242	0.936	1

[a] R_s is the ohmic resistance of the solution between electrode and point located on the axis of the disk at distance z from the electrode. R_{max} is the ohmic resistance of the solution at a point located on the axis at the distance of $10r_d$ from the electrode.

concentrations, participates in both the diffusion and the migration processes. Moreover, we are using the rotating disk electrode, which produces high values of the liquid−solid mass transfer coefficient.

We now show, with more detailed calculations, that in the present case, diffusion does not limit the current density. The expression for the diffusion limiting current density on rotating disk electrode is given by Levich[76]

$$i_d = 0.62FD^{2/3}\omega^{1/2}\nu^{-1/6}c_{NaCl} \quad (21)$$

where D is the diffusion coefficient, ω is the speed of rotation of the electrode $(\mathrm{rad\cdot s^{-1}})$, ν is the kinematic viscosity of the solution $\mathrm{m^2\cdot s^{-1}}$, and c_{NaCl} is the bulk concentration of NaCl solution $(\mathrm{mol\cdot m^{-3}})$. We use the following data to estimate the diffusion limiting current: concentration of NaCl 1 M (c_{NaCl} = 1000 $\mathrm{mol\cdot m^{-3}}$), ω = 251 $\mathrm{rad\cdot s^{-1}}$, $D_{Cl^-} = 2.03 \times 10^{-9}$ $\mathrm{m^2\cdot s^{-1}}$, $\nu = 10^{-6}$ $\mathrm{m^2\cdot s^{-1}}$. This gives i_d = 15.2 $\mathrm{kA\cdot m^{-2}}$. Moreover, in the present case, since both migration and diffusion occur in parallel in the diffusion film, the actual limiting current density is approximately twice the value of i_d, thst is, 30 $\mathrm{kA.m^{-2}}$. This value is much larger than the highest value of 9.2 $\mathrm{kA\cdot m^{-2}}$, which is actually observed in our experiments (see Figure 7). That the diffusion limit is not reached in our experiments is also evident from Figure 5, which shows that the current density is independent of the speed of the rotation of disk electrode.

It is not possible to eliminate the ohmic drop by appropriate placement of the Luggin capillary. The reason being, the major ohmic resistance is located within one disk radius. Table 1 presents the values of the ohmic resistance at different location on the axis of the disk. It is computed by Newman[75] based on the solution of the Laplace equation around a disk electrode.

It is seen from this table that most of the ohmic resistance is located within the distance equal to half the radius of the electrode (i.e., z = 1.25 mm in the present case). The reason is that the current converges on the disk. Therefore, the current density increases rapidly as we approach the disk. An attempt to reduce the ohmic resistance would necessitate placing of the tip of the Luggin capillary very close to the electrode. This would disturb the potential distribution around the electrode and thereby modify the ohmic resistance in an unpredictable manner. It is therefore preferable to place the Luggin capillary at least one radius away from the disk and estimate the ohmic resistance using eq 11.

We can now explain some of the experimental observations presented in the previous section. In the chronoamperograms in Figure 8, we find that the current density remains constant for certain period of time and then begins to decrease. This transition can be explained as follows. In the beginning, the electrode is very active and the exchange current density is high enough to satisfy the condition $i_0(F/RT)A_eR_S \gg 1$. Equation 17 is valid in this period. Moreover, since the electrode potential is held constant, the current density also remains constant. As the

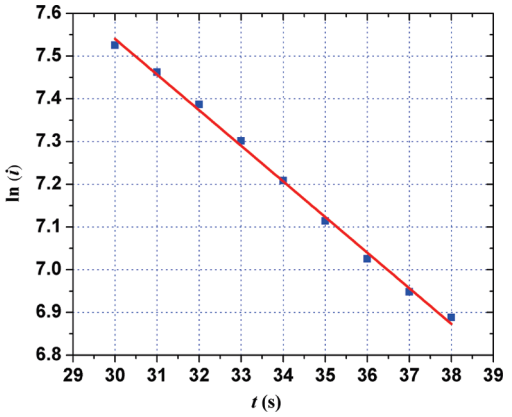

Figure 10. Plot of ln i versus time on platinum electrode undergoing passivation in the fast regime. Data are taken from that plot in Figure 8, where the electrode is held at a potential of 1.85 V. Parameters: speed of rotation of disk, 50 Hz; concentration of NaCl, 1 M; reference electrode, saturated calomel. Current density is in $\mathrm{A\cdot m^{-2}}$.

electrode continues to passivate, a point is reached when $i_0(F/RT)A_eR_S$ is comparable to unity and current then begins to fall below the value estimated by eq 17. This marks the end of the constant current period. The length of this period depends on the rate at which the electrode passivates, that is, the rate at which i_0 decreases with time. Greater the rate, shorter is the period. Since, the rate of passivation increases with increase in the electrode potential, the constant current period decreases with increase in the potential. This trend is evident from Figure 8.

The reverse sweep voltammogram of Figure 9, for a freshly activated electrode is a straight line right down to V_{eq}. This is consistent with eq 17, which is true for a highly active electrode. As the passivation develops, the reverse sweep voltammogram becomes increasingly nonlinear. The voltammogram then follows the conventional Butler−Volmer equation until $i\alpha(F/RT)A_eR_S$ is comparable to unity and then transits to the migration regime. As the electrode passivates, increasingly greater potential is needed before this transition occurs. This is also evident from this figure.

5.7. Modeling the Fast Regime of Passivation of Platinum Electrode. In Figure 8, the two regimes of passivation are evident, namely, fast and slow. We postulate that the fast regime corresponds to formation of the oxide monolayer. Here, the surface atoms of platinum are oxidized. During the second regime, the surface activity is sustained by diffusion and migration of oxygen ions from the surface into the lattice space of the metal. This process slows down the rate of passivation. We support these claims based on our experimental findings.

In this section, we discuss the fast regime of passivation. We assume that the surface of the electrode is composed of two types of sites, the metal sites and the oxide sites. If the fraction of the area occupied by the oxide sites is denoted by θ, then the fraction of the area occupied by active metal sites would be $1 - \theta$. If we assume that the rate of passivation is first order in the concentration of the active metal sites, we can write the equation describing the passivation process as

$$\frac{d\theta}{dt} = k_f(1 - \theta) \quad (22)$$

Here, k_f represents the rate constant for passivation during the fast regime. It is expected to depend on the electrode potential.

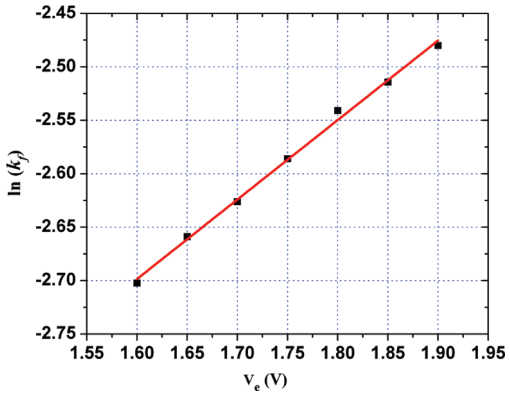

Figure 11. Plot of ln k_f versus electrode potential The values of k_f (s^{-1}) are obtained from the slopes of ln(i) vs time plots as presented in Figure 10. The data $i-t$ are derived from Figure 8.

Since the current density for the chloride ion oxidation is proportional to the concentration of the active sites, we can write

$$i = k_0(1 - \theta) \tag{23}$$

where k_0 is constant. Replacing θ by i in eq 22 using eq 23, and integrating the resulting equation, we obtain the following expression relating current density and time

$$\ln i = k_f t + c \tag{24}$$

This equation implies that the logarithm of current density varies linearly with time during the fast passivation regime. To test this model, we have chosen the regions of the chronoamperograms in Figure 8, where there is the steepest fall in the current. A typical plot of ln$i$ versus time in the steepest region is shown in Figure 10. Here the electrode potential is held at 1.85 V. The plot is a straight line with slope of $-0.0809\ s^{-1}$. This gives $k_f = 0.0809\ s^{-1}$. The value c is 9.96.

Since the electrode passivates by electrochemical reaction with water, we expect k_f to depend exponentially on electrode potential. This expectation is verified in Figure 11, which plots ln k_f versus the electrode potential. The plot is a straight line, indicating exponential dependence.

The slope of the plot is 0.744 and the intercept on ln k_f axis is -3.889. Hence, we can write the passivation rate constant k_f as

$$k_f = 0.2047 \exp(0.774 V_e) \tag{25}$$

We can now express the current density during fast passivation regime by combining eq 24 and 25. Thus

$$\ln i = -0.2047 t \exp(0.774 V_e) + c \tag{26}$$

The intercept c represents the current density at zero time, that is, $c = \ln i|_{t=0}$. Note that $i|_{t=0}$ is the current density on the freshly activated electrode. The values of ln $i|_{t=0}$ and $i|_{t=0}$ at different electrode potentials are listed in Table 2

It is seen from Table 2 that when the electrode is in the active state, the current density is very high. This is expected. The apparently odd observation is that ln $i|_{t=0}$ decreases with increase in the electrode potential. We should however note that in these experiments, the electrode is preactivated at -2 V. Its potential is then reset at the desired passivation potential and the current is recorded as function of time. The electrode undergoes passivation during the process of resetting the electrode from the activation potential to passivation potential. Greater the passivation potential, greater is the extent of passivation during the resetting period.

Table 2. Current Densities at Active Platinum Electrode[a]

potential (V)	ln $i\|_{t=0}$	$i\|_{t=0}$ ($A \cdot m^{-2}$)
1.6	23.40	1.45×10^{10}
1.65	20.21	5.98×10^{8}
1.7	17.77	5.21×10^{7}
1.75	16.06	9.43×10^{6}
1.80	13.21	5.45×10^{5}
1.85	9.96	2.12×10^{4}
1.90	9.53	1.37×10^{4}

[a] The values of ln $i|_{t=0}$ are obtained by extending the plot of ln i versus t (see Figure 10) to $t = 0$.

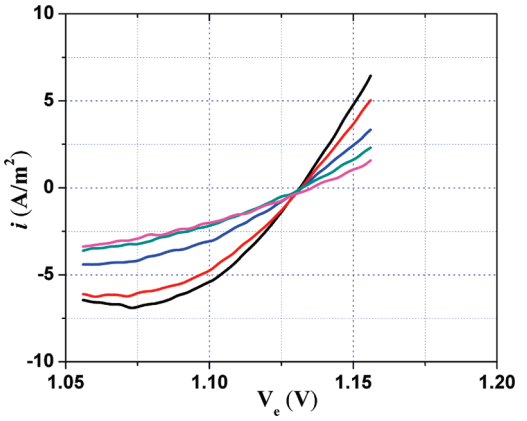

Figure 12. Voltammograms for chloride ion oxidation on platinum electrode passivated for different durations of time. (Only the portions of the voltammograms in the vicinity of equilibrium potential are shown.) Parameters: concentration of NaCl, 1 M; speed of rotation of disk, 50 Hz; potential range, 2.0−0 V; scan rate, 1500 $mV \cdot s^{-1}$. Line colors correspond to duration of passivation: black, 8.0 s; red, 8.5 s; blue, 9.0 s; green, 12 s; magenta, 13.5 s.

The Table 2 reveals two important points. First, the freshly activated electrode is extremely active. Second, its rate of deactivation is also very fast. Both these factors would make the direct estimation of the activity of freshly conditioned platinum electrode an extremely difficult task.

5.8. Modeling the Slow Regime of Passivation of Platinum Electrode. We have fitted those reverse sweep voltammograms of Figure 9 which correspond to slow passivation regime (passivation times of 8 s and longer), using the Tafel form of eq 15. The data analyzed also include voltammograms corresponding to very long passivation times which are not included in Figure 9. The parameters in the equation are i_0, V_{eq}, α, and R_S. To check whether the value of V_{eq} is affected by passivation, we have plotted, in Figure 12, those portions of the reverse sweep voltammograms of Figure 9, which are in the vicinity of V_{eq}. It is seen that all curves pass through a single value of V_{eq} of 1.131 V, indicating that the mechanism of oxidation does not change during the passivation process. We also expect the value of α to be the same for all voltammograms. The value of R_S is also known a priori. This leaves only two unknown parameters, namely, i_0 and α. Between these two parameters, α is common to all voltammograms. Only i_0 is specific to each curve.

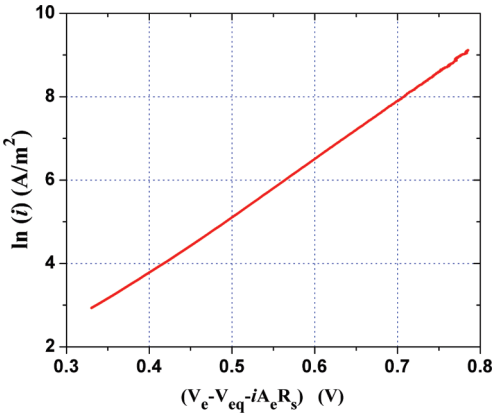

Figure 13. Tafel region of typical reverse sweep voltammogram on a passivated platinum electrode (passivation time and potential 600 s and 2.0 V). Parameter: concentration of NaCl, 1 M; speed of rotation, 50 Hz; scan rate, 1500 mV·s^{-1}.

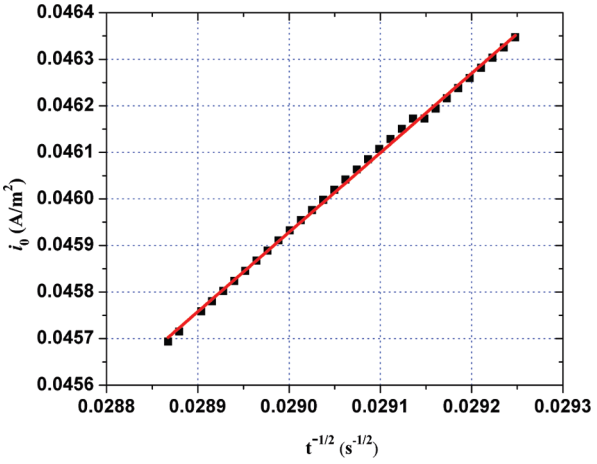

Figure 14. Plot of exchange current density for chloride ion oxidation versus inverse square root of time. Parameter: concentration of NaCl, 1 M; speed of rotation of disk, 50 Hz; potential, 1.75 V.

At intermediate potentials, eq 15 reduces to the Tafel equation

$$i = i_0 \exp\left[\alpha \frac{F}{RT}(V_e - V_{eq} - iA_eR_s)\right] \quad (27)$$

Applying logarithm on both sides, we get

$$\ln(i) = \ln(i_0) + \frac{\alpha F}{RT}(V_e - V_{eq} - iA_eR_s) \quad (28)$$

The plot of $\ln(i)$ versus $(V_e - V_{eq} - iA_eR_S)$ should be a straight line having slope $\alpha F/RT$.

A typical Tafel plot (corresponding to passivation the time of 600s at 2 V potential) is shown in Figure 13. It is a straight line having slope of 13.8 and intercept of −1.77 on $\ln(i)$ axis. From these, we estimate the value of α as 0.36 and that of i_0 as 0.171 A·m^{-2}.

In Figure 14, we show a plot of the exchange current density versus $t^{-1/2}$ for passivation at 1.75 V. The plot is straight line having a slope of 1.65 A·m^{-2}·s$^{0.5}$ and intercept on i_0 axis of 1.9×10^{-3}A·m^{-2}. Similar plots are drawn for other potentials. The corresponding slopes and the intercepts are listed in Table 3.

This trend of the exchange current density is explained on the basis of the model for passivation. We assume that during the slow passivation regime, practically all the electrode surface is covered by oxide sites. Oxygen ions move through the metal lattice by the place-exchange mechanism.[62] This movement of ions results in reactivation of the platinum atoms on the surface of the metal, thereby partially restoring the activity of the electrode. The movement of ions is caused by both diffusion and migration through the metal. We can also view this process as movement of oxide sites. The flux of oxide sites N_θ is given by the Nernst−Planck equation as

Table 3. Values of Slope and Intercept of Plots of i_0 vs $t^{-1/2}$ at Various Electrode Potentials[a]

potential (V)	slope $2(i_{0m}/k_p)(D/\pi)^{1/2}$ (A·m^{-2}·s$^{1/2}$)	intercept i_{0o} (A·m^{-2})
1.6	3.84	3.5×10^{-2}
1.65	2.67	1.4×10^{-2}
1.7	2.00	5.7×10^{-3}
1.75	1.65	1.9×10^{-3}
1.80	1.37	6.5×10^{-4}
1.85	1.02	3.2×10^{-3}

[a] See eq 33 for the interpretation of the slope and that intercept.

$$N_\theta = -D\frac{\partial\theta}{\partial z} - Zu\theta F\frac{\partial V}{\partial z} \quad (29)$$

where D and u are the diffusion coefficient and migration coefficient for the oxide site through the lattice, z is the distance measured from the surface into the metal, and Z is the valency of oxygen ion (= 2). We now show that the contribution to the total flux due to migration is much smaller than that due to diffusion. For the highest value of the current density of $i = 4000$ A·m^{-2}, the field across the oxide film is $\partial V/\partial z = i/\kappa = 4000/0.1 = 4 \times 10^4 V \cdot m^{-1}$. Use of Nernst−Einstein equation, that is, $u = D/RT$ allows us to express the ratio of the diffusion flux to the migration flux as $(RT/ZF)(\partial\theta/\partial z)/(\theta\,\partial V/\partial z)$. Using $\theta = 1$, $z = 10^{-10}$ m, we obtain the ratio of the fluxes as 3.2×10^3, indicating that only the diffusion flux is important.

The diffusion equation for the oxide sites can be written as

$$\frac{\partial\theta}{\partial t} = D\frac{\partial^2\theta}{\partial z^2} \quad (30)$$

where D is the diffusion coefficient for the oxide site through the lattice, z is the distance measured from the surface into the metal, and t is time.

We now assume that the rate of change of the concentration of the oxide sites on the surface is slow enough to allow us to use quasi-steady state assumption. Thus the surface concentration of oxide sites θ^* can be assumed as constant while solving eq 30. This equation then gives the following solution, subject to boundary conditions $\theta = \theta^*$ at $z = 0$ and $\theta = 0$ as $z \to \infty$

$$\frac{\theta}{\theta^*} = 1 - \mathrm{erf}\left(\frac{z}{\sqrt{Dt}}\right) \quad (31)$$

The diffusive flux of the oxide sites at the surface is given by

$$N_\theta = -D\left.\frac{\partial\theta}{\partial z}\right|_{z=0} = 2\theta^*\sqrt{\frac{D}{\pi t}} \quad (32)$$

The rate of generation of the oxide sites by oxidation of platinum by water is given by $k_p(1 - \theta^*)$, where k_p is the rate

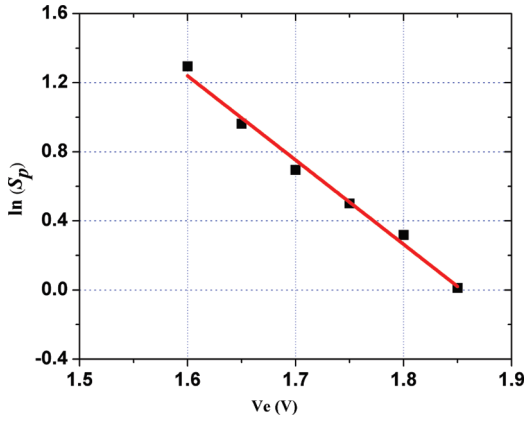

Figure 15. Plot of $\ln(s_p)$ versus the electrode potential (the values of s_p are obtained from Table 3). Parameters: concentration of NaCl, 1 M; speed of rotation of disk, 50 Hz.

constant for passivation and $(1 - \theta^*)$ is the fraction of the area occupied by metal sites.

Equating the rate of generation of oxide sites with their rate of diffusion, we get

$$\theta^* = \frac{k_p}{k_p + 2\sqrt{D/\pi t}} \tag{33}$$

Note that the θ^* is the function of time as seen from eq 33. However, its variation with time is very small since most of the surface sites are in the oxidized state so that value of θ^* is nearly equal to unity.

The exchange current density for chloride oxidation reaction can now be written as

$$i_0 = i_{0m}(1 - \theta^*) + i_{0o}\theta^* \approx i_{0m}(1 - \theta^*) + i_{0o} \tag{34}$$

where i_{0m} is the exchange current density for chloride oxidation on metal sites and i_{0o} is that on the oxide sites.

Substituting the expression for θ^* from eq 33 into eq 34, we get

$$i_0 = i_{0o} + i_{0m}\frac{2\sqrt{D/\pi t}}{k_p + 2\sqrt{D/\pi t}} \tag{35}$$

If $k_p \gg 2(D/\pi t)^{1/2}$, then eq 35 reduces to

$$i_0 = i_{0o} + 2\left(\frac{i_{0m}}{k_p}\right)\sqrt{D/\pi t} \tag{36}$$

Thus, the plot of the exchange current density i_0 versus $1/(t)^{1/2}$ is a straight line with slope $2(i_{0m}/k_p)(D/\pi)^{1/2}$ and the intercept i_{0o}.

The slope of the plot in Figure 14 is $s_p = 2(i_{0m}/k_p)(D/\pi)^{1/2}$. It is a composite of three terms. Among them, k_p is the rate constant for oxidation of the metal sites. It depends on potential. We can express it in the Tafel form as

$$k_p = \frac{i_p}{F} = \frac{i_{0p}}{F}e^{(\alpha_p F/RT)V_e} \tag{37}$$

Substituting this expression in the expression for s_p, we get

$$s_p = 2F\left(\frac{i_{0m}}{i_{0p}}\right)(e^{-(\alpha_p F/RT)V_e})\sqrt{D/\pi} \tag{38}$$

Hence plot of $\ln(s_p)$ versus V_e should be a straight line with slope $-\alpha_p F/RT$ and the intercept on y-axis of $\ln(2F(i_{0m}/i_{0p})(D/\pi)^{1/2})$.

Figure 15 shows this plot, which is based on the data of Table 3. The slope of the plot is $-4.87\ V^{-1}$, and the intercept is 9.04.

From the slope, the value α_p can be computed as 0.13. From the intercept, we obtain the value of $(i_{0m}/i_{0p})\sqrt{D}$ as 7.78×10^{-2} $m \cdot s^{-1/2}$. Schmiedl et al.[77] have measured diffusivity of oxygen through thin platinum films deposited on silicon wafers. Their estimate of the diffusion coefficient is $D \approx 10^{-23}\ m^2 \cdot s^{-1}$. Using this value of D, we can estimate the ratio of i_{0m}/i_{0p} as approximately 10^{10}. A rough estimate of the exchange current density on the electrode undergoing passivation, i_{0p}, can be obtained as follows. From Figure10, we see that the rapid passivation phase lasts for about 10 s in which a monolayer of oxide is formed. Since platinum surface contains approximately 10^{19} molecules per square meter, we can compute the charge required to form the monolayer as about $1\ C \cdot m^{-2}$. From this charge, we can get the approximate value of the passivation current density as $i_p \approx 0.1$ $A \cdot m^{-2}$. Using eq 37, we can estimate the magnitude of i_{0p} as about $10^{-6}\ A \cdot m^{-2}$. This gives us the rough estimate of i_{0m} as 10^5 $A \cdot m^{-2}$. From this we can calculate the current density which is expected on the active electrode kept at a potential of 2 V.

$$i_m = i_{0m}\exp\left\{\alpha\frac{F}{RT}(V_e - V_{eq})\right\} \approx 10^{10}\ A \cdot m^{-2} \tag{39}$$

Here, we have used $\alpha = 0.36$, $V_{eq} = 1.131$ V, and $V_e = 2.0$ V. This value i_m should compare with $i|_{t=0}$ reported in Table 1. We see that order of magnitude compares well with the value for V_e = 1.6 V. This is not surprising since this value in Table 1 corresponds to most active state of the electrode.

The magnitude of the exchange current density on oxide sites, i_{0o}, as seen in Table 1, lie in the range of 10^{-3} to $10^{-2}\ A \cdot m^{-2}$. We expect i_{0o} to be constant. The scatter is caused by high sensitivity of the intercept to the portion of the chronoamperograms selected for fitting. However, we see that the magnitude of i_{0o} is too small so that the second term of eq 36, which corresponds to the contribution by the active sites, dominates the total current density for very long time (of the order of 10 ks.)

CONCLUSIONS

We can see from this analysis that the, kinetics of chloride oxidation in a concentrated aqueous solution of NaCl can be described by Butler−Volmer equation, in which the ohmic resistance of the solution is incorporated. When the electrode is very active, the magnitude of the exchange current density i_0 is very high and hence the current is solely controlled by the ohmic resistance. Electrode, however, undergoes passivation. Two passivation regimes are observed. In the fast passivation regime, the current density decays due to oxidation of surface sites. The decay is exponential with time according to the equation

$$\ln\left(\frac{i}{i|_{t=0}}\right) = -0.2047t\exp(0.774V_e) \tag{40}$$

The values of $i|_{t=0}$, the current density at zero time, decreases with increase in the passivation potential. This decrease is attributed to the fact that the electrode is in a partially passivated state even at the beginning of the experiment. However, we find that on an active electrode, the current density would be at least $10^{10}\ A \cdot m^{-2}$ at the electrode potential of about 1.6 V.

During the slow passivation regime, the current density can be described by the Butler−Volmer equation with V_{eq} = 1.131 V and the transfer coefficient of α = 0.36. The exchange current

density varies inversely with square root of time due to passivation. It is describe by the following equation, which is derived by combining eq 33 and 34.

$$i_0 = i_{0o} + 2F\left(\frac{i_{0m}}{i_{0p}}\right)\left(e^{-(\alpha_p F/RT)V_e}\right)\sqrt{D/\pi t} \quad (41)$$

This square root dependence arises due to diffusion of oxygen ions from the surface to the metal bulk. The value of $(i_{0m}/i_{0p})\sqrt{D}$ as 7.78×10^{-2} m·s$^{-1/2}$, and the value of α_p 0.13. The magnitude of i_{0o}, the exchange current density on oxide sites, is in the range of 10^{-3}—10^{-2} A·m^{-2}. The contribution to the total current by the oxide sites is very small compared to the contribution from the metal sites.

AUTHOR INFORMATION

Corresponding Author

*Tel: +91-22-25767236. Fax: +91-22-25766895. E-mail: vaj@iitb.ac.in.

ACKNOWLEDGMENT

Authors wish to acknowledge Unilever Industries Private Limited, Bangalore, India for funding this research.

NOMENCLATURE

A_e = area of the disk electrode, m^2
a_{Cl^-} = activity of the chloride ion
c_{NaCl} = concentration of sodium chloride, M
D = diffusion coefficient for the oxide site, m^2·s^{-1}
E = Nernst potential, V
E^0 = standard electrode potential, V
F = Faraday constant, C·mol^{-1}
i = current density, A·m^{-2}
i_d = diffusion limiting current density, A·m^{-2}
i_m = current density on active platinum surface, A·m^{-2}
i_0 = exchange current density, A·m^{-2}
i_{0m} = exchange current density on active platinum sites, A·m^{-2}
i_{0o} = exchange current density on platinum oxide sites, A·m^{-2}
i_{0p} = exchange current density on passive platinum, A·m^{-2}
K = equilibrium constant of reaction of chlorine with water, M^2
K_a = dissociation constant of HOCl
k_f = rate constant for passivation in fast regime, s^{-1}
k_p = rate constant for passivation in slow regime, mol·m^{-2}·s^{-1}
N_θ = flux of oxide sites, mol·m^{-2}·s^{-1}
n = number of electron transferred
p_{Cl_2} = partial pressure of the chlorine gas, Pa
R = universal gas constant, J·mol^{-1}·K^{-1}
R_s = solution resistance, ohm
r_d = radius of the disk electrode, m
T = temperature, K
t = time, s
u = migration coefficient of oxygen ion, m^2·mol·s^{-1}·J^{-1}
V_e = electrode potential, V
V_{eq} = equilibrium electrode potential, V
V_e^m = threshold potential for transition to migration controlled regime, V
z = valency of oxygen ion
α = transfer coefficient in eq 13
α_p = transfer coefficient in eq 32
η = overpotential, V
κ_e = conductivity of NaCl solution estimated using eq 12, S·m^{-1}
κ_m = measured conductivity of NaCl solution, S·m^{-1}
ν = kinematic viscosity of the solution, m^2·s^{-1}
θ = fraction of the sites in the oxide form
θ^* = value of θ on the electrode surface
ω = angular velocity of the rotating disk electrode, rad·s^{-1}

REFERENCES

(1) White, G. C. *Handbook of Chlorination*; Van Nostrand Reinhold Company Inc.: New York, 1986; pp. 150, 203.
(2) Kraft, A. Electrochemical Water Disinfection: A Short Review. *Platinum Met. Rev.* **2008**, *52*, 177.
(3) Kraft, A.; Stadelmann, M.; Blaschke, M.; Kreysig, D.; Sandt, B.; Schroder, F.; Rennau, J. Electrochemical Water Disinfection Part I: Hypochlorite Production from Very Dilute Chloride Solutions. *J. Appl. Electrochem.* **1999**, *29*, 859.
(4) Szpyrkowicz, L.; Juzzolino, C.; Kaul, S. N. A Comparative Study on Oxidation of Disperse Dyes by Electrochemical Process, Ozone, Hypochlorite, and Fenton Reagent. *Water Res.* **2001**, *35*, 2129.
(5) Smith, W. ;Leslie, S. Reversible Polarity Electrode System. Int. Patent WO 2006/058369 A1, 2006.
(6) Hayfield, P. C. S. Development of the Noble Metal/Oxide Coated Titanium Electrode. *Platinum Met. Rev.* **1998**, *42*, 27.
(7) Hayfield, P. C. S. Development of the Noble Metal/Oxide Coated Titanium Electrode. *Platinum Met. Rev.* **1998**, *42*, 116.
(8) Hayfield, P. C. S. Development of the Noble Metal/Oxide Coated Titanium Electrode. *Platinum Met. Rev.* **1998**, *42*, 46.
(9) Kraft, A. Doped Diamond: A Compact Review on a New Versatile Electrode Material. *Int. J. Electrochem. Sci.* **2007**, *5*, 355.
(10) Patermarakis, G.; Fountoukidis, E. Disinfection of Water by Electrochemical Treatment. *Water Res.* **1990**, *24*, 1491.
(11) Arikado, T.; Iwakura, C.; Tamura, H. Chlorine Evolution Reaction on Platinum and Several Alloys. *Electrochim. Acta* **1977**, *22*, 229.
(12) Frumkin, A. N.; Tadoradze, G. A. The Mechanism of Ionization of Molecular Chlorine at a Platinum Electrode. *Z. Elektrochem.* **1958**, *62*, 251.
(13) Tedoradze, G. A. Oxidation Kinetics of Chloride Ions on Platinum. *Zh. Fiz. Khim.* **1959**, *33*, 129.
(14) Chang, F. T.; Wick, H. Halogen Overvoltage. *Z. Phys. chem.* **1935**, *A172*, 448.
(15) Thomassen, M.; Borresen, B.; Hagen, G.; Tunold, R. Chlorine Reduction on Platinum and Ruthenium: The Effect of Oxide Coverage. *Electrochim. Acta* **2005**, *50*, 1157.
(16) Tilak, B. V. Kinetics of Chlorine Evolution-A Comparative Study. *J. Electrochem. Soc.* **1979**, *126*, 1343.
(17) Conway, B. E.; Novak, D. M. Electrocatalytic Effect on the Oxide Film at Pt Anodes on Cl* Recombination Kinetics in Chlorine Evolution. *J. Electroanal. Chem.* **1979**, *99*, 133.
(18) Dickinson, T.; Greef, R.; Wynne-Jones, L. The Kinetics of the Chlorine Electrode Reaction at a Platinum Electrode. *Electrochim. Acta* **1969**, *14*, 467.
(19) Burrows, I. R.; Entwisle, J. H.; Harrison, J. A. The Mechanism of Oxidation of Chloride Ions on Platinum and Ruthenium(IV) Oxide/Titanium Oxide Electrodes, and the Reduction of Molecular Chlorine on Platinum. *J. Electroanal. Chem. Interfacial Electrochem.* **1977**, *77*, 21.
(20) Hoar, T. P. The Mechanism of the Oxygen Electrode. *Proc. R. Soc.* **1933**, *A142*, 628.
(21) Bockris, J. O. M. Kinetics of Activation Controlled Consecutive Electrochemical Reactions: Anodic Evolution of Oxygen. *J. Chem. Phys.* **1956**, *24*, 817.
(22) Hoare, J. P. Oxygen Overvoltage Measurements on Bright Platinum in Acid Solutions. *J. Electrochem. Soc.* **1965**, *112*, 602.
(23) Hoare, J. P. Oxygen Overvoltage Measurements on Bright Platinum in Acid Solutions. *J. Electrochem. Soc.* **1965**, *112*, 849.

(24) Rozental, K. I.; Veselovskii, V. I. Investigation with Oxygen-18 of the Electrochemical Oxygen Evolution Mechanism on Platinum Electrodes. *Dokl. Akad. Nauk SSSR* **1956**, *111*, 637.
(25) Bagotskii, V. S.; Yablokova, E. I. Mechanism of Electrochemical Reduction of Oxygen and Hydrogen Peroxide on a Mercury Electrode. *Zh. Fiz. Khim.* **1953**, *27*, 1663.
(26) Krasilshchikov, A. I. Intermediate Stages in the Anodic Evolution of Oxygen. *Zh. Fiz. Khim.* **1963**, *37*, 531.
(27) Bockris, J. O. M.; Shamshul Huq, A. K. M. The Mechanism of the Electrolytic Evolution of Oxygen on Platinum. *Proc. R. Soc.* **1956**, *A237*, 271.
(28) Conway, B. E.; Bourgault, P. L. Electrochemistry of the Nickel Oxide Electrode Part III Anodic Polarization and Self Discharged. *Can. J. Chem.* **1962**, *40*, 1960.
(29) Conway, B. E.; Gileadi, E. Electrochemistry of the Nickel Oxide Electrode Part IV: Electrochemical Kinetic Studies of Reversible Potential as a Function of Degree of Oxidation. *Can. J. Chem.* **1962**, *40*, 1933.
(30) Riddiford, A. C. Mechanisms for the Evolution and Ionization of Oxygen at Platinum Electrodes. *Electrochim. Acta* **1961**, *4*, 170.
(31) amjanovic, A. D.; Bockris, J. O. M. Kineics of Oxygen Evolution and Dissolution on Platinum Electrodes. *Electrochim. Acta* **1966**, *11*, 791.
(32) Robertson, R. D. The Capacity of Polarized Platinum Electrodes in Hydrochloric Acid. *J. Electrochem. Soc.* **1953**, *100*, 194.
(33) Popat, P. V.; Hackerman, N. Capacity of the Electric Double Layer and Adsorption at Polarized Platinum Electrodes: Adsorption of Anions. *J. Phys. Chem.* **1958**, *62*, 1198.
(34) Schwabe, K. Untersuchung Uber Die Anionenadsorption Mit Hilfe Markierter Ionen. *Electrochim. Acta* **1962**, *6*, 223.
(35) Breiter, M. Uber Die Art Der Wasserstoffadsorption An Platinmetallelektroden. *Electrochim. Acta* **1962**, *7*, 25.
(36) Sarmousakis, J. N.; Prager, J. M. Impedance at Polarized Platinum Electrodes in Various Electrolytes. *J. Electrochem. Soc.* **1957**, *104*, 454.
(37) Wicke, E.; Weblus, B. Capacity of Polarization, Adsorption, and Overvoltage on Platinum. *Z. Elektrochem.* **1952**, *56*, 169.
(38) Lorenz, W.; Muhlberg, H. Measurements of the Absorption of Potential-Determining Ions on Electrodes by the Method of Nonstationary Concentration Polarization. *Z. Elektrochem.* **1955**, *59*, 736.
(39) Balashova, N. A. Determination of the Ion Adsorption and of the Zero Potential by Aid of Labeled Atoms. *Z. Physik. Chem.* **1957**, *207*, 340.
(40) Obrucheva, A. D. Investigation of Ion Adsorption on Platinized Platinum by Measurements of Adsorption Potentials. *Zh. Fiz. Khim.* **1958**, *32*, 2155.
(41) Birinzeva, T. P.; Kabanov, B. N. Alternating-Current Method of Anion-Adsorption Measurement on Platinum. *Zh. Fiz. Khim.* **1959**, *33*, 844.
(42) Balashova, N. A. Einfluss Des Zustandes Der Oberflache Auf Die Ionenadsorption Am Platin. *Electrochim. Acta* **1962**, *7*, 559.
(43) Breiter, M. W. Voltammetric Study of Halide Ion Adsorption on Platinum in Perchloric Acid Solutions. *Electrochim. Acta* **1963** *8*, 925.
(44) Gilman, S. Studies of Anion Adsorption on Platinum by the Multipulse Potentiodynamic (M.p.p.) Method. I. Kinetics of Chloride and Phosphate Adsorption and Associated Charge at Constant Potential. *J. Phys. Chem.* **1964**, *68*, 2098.
(45) Gilman, S. Studies of Anion Adsorption on Platinum by the Multipulse Potentiodynamic (M.p.p.) Method. II. Chloride and Phosphate Desorption and Equilibrium Surface Concentrations at Constant Potential. *J. Phys. Chem.* **1964**, *68*, 2112.
(46) Li, F. B.; Robert Hillman, A.; Lubetkin, S. D.; Roberts, D. J. Electrochemical Quartz Crystal Microbalance Studies of Potentiodynamic Electrolysis of Aqueous Chloride Solution: Surface Processes and Evolution of H_2 and Cl_2 Gas Bubbles. *J. Electroanal. Chem.* **1992**, *335*, 345.
(47) Wang, L. P.; Bassiri, M. P.; Najafi, R. P.; Najafi, K. M.; Yang, J. B. S.; Khosrovi, B. P.; Hwang, W. B.; Belisle, B. P.; Celeri, C. M.; Robson, MC. M. Hypochlorous Acid as a Potential Wound Care Agent Part I: Stabilized Hypochlorous Acid: A Component of the Inorganic Armamentarium of Innate Immunity. *J. Burns. Wound* **2007**, *6*, 65.
(48) Czarnetzki, L. R.; Janssen, L. J. J. Formation of Hypochlorite, Chlorate and Oxygen During NaCl Electrolysis from Alkaline Solutions at an RuO_2/TiO_2 Anode. *J. Appl. Electrochem.* **1992**, *22*, 315.
(49) Anson, F. C.; Lingane, J. J. Chemical Evidence for Oxide Films on Platinum Electrometric Electrodes. *J. Am. Chem. Soc.* **1957**, *79*, 4901.
(50) Hickling, A.; Wilson, W. H. The Anodic Decomposition of Hydrogen Peroxide. *J. Electrochem. Soc.* **1951**, *98*, 425.
(51) Laitinen, H. A.; Enke, C. G. The Electrolytic Formation and Dissolution of Oxide Films on Platinum. *J. Electrochem. Soc.* **1960**, *107*, 773.
(52) Bold, W.; Breiter, M. Untersuchung des anodischen aufbaus und der kathodischen reduktion der sauerstoffbelegung an glatten pt-elektroden. *Electrochim. Acta* **1961**, *5*, 145.
(53) Bowden, F. P. The Amount of Hydrogen and Oxygen Present on the Surface of a Metallic Electrode. *Proc. R. Soc.* **1929**, *A125*, 446.
(54) Butler, J. A. V.; Armstrong, G. The Electrolytic Properties of Hydrogen. Part I. Hydrogen as an Anodic Depolariser. Part II. Effect of Anodic Polarisation of the Platinum Electrodes. *J. Chem. Soc.* **1934**, 743.
(55) Gilman, S. Electrochemical Surface Oxidation of Platinum. *Electrochim. Acta* **1964**, *9*, 1025.
(56) Biegler, T.; Woods, R. Limiting Oxygen Coverage on Smooth Platinum Anodes in Acid Solution. *J. Electroanal. Chem. Interfacial Electrochem.* **1969**, *20*, 73.
(57) Feldberg, S. W.; Enke, G. C.; Bricker, G. S. Formation and Dissolution of Platinum Oxide Film: Mechanism and Kinetics. *J. Electrochem. Soc.* **1963**, *110*, 826.
(58) Hoare, J. P. In *The Electrochemistry of Oxygen*; John Wiley and Sons: New York, 1968; p 13.
(59) Thacker, R.; Hoare, J. P. Sorption of Oxygen from Solution by Noble Metals: I. Bright Platinum. *J. Electroanal. Chem. Interfacial Electrochem.* **1971**, *30*, 1.
(60) Goswami, K. N.; Staehle, R. W. Growth Kinetics of Passive Films on Fe, Fe-Ni, Fe-Cr, Fe-Cr-Ni Alloys. *Electrochim. Acta* **1971**, *16*, 1895.
(61) Cabrera, N.; Mott, N. F. Theory of Oxidation of Metals. *Rep. Prog. Phys.* **1949**, *12*, 163.
(62) Norio, S.; Morris, C. The Kinetics of Anodic Oxidation of Iron in Neutral Solution. *J. Electrochem. Soc.* **1964**, *111*, 512.
(63) Sato, N.; Notoya, T. Measurement of the Anodic Oxide Film Growth on Iron for Hours. *J. Electrochem. Soc.* **1967**, *114*, 585.
(64) Fehlner, F. P.; Mott, N. F. Low-Temperature Oxidation. *Oxid. Met.* **1970**, *2*, 59–99.
(65) Chao, C. Y.; Lin, L. F.; Macdonald, D. D. A Point Defect Model for Anodic Passive Film I. Film Growth Kinetics. *J. Electrochem. Soc.* **1981**, *128*, 1187.
(66) Shibata, S. Conductance Measurement of Thin Oxide Films on a Platinum Anode. *Electrochim. Acta* **1977**, *22*, 175.
(67) Littauer, E. L.; Shreir, L. L. Anodic Polarization of Platinum in Sodium Chloride Solutions. *Electrochim. Acta* **1966**, *11*, 527.
(68) Glasstone, S.; Hickling, A. Studies in Electrolytic Oxidation. Part IV. Anodic Polarisation in Halide Solutions. *J. Chem. Soc.* **1934**, 10.
(69) Grube, G. Anodic and Kathodic Retardation Phenomena and their Bearing upon the Theory of Passivity. *Trans. Faraday Soc.* **1914**, *9*, 214.
(70) Obrucheva, D. The Platinum Electrode. X. Study of the Adsorption of Oxygen by Smooth Platinum by the Electrochemical Method. *Zh. Fiz. Khim.* **1952**, *26*, 1448.
(71) Hickling, A. The Anodic Behaviour of Metals. Part I.-Platinum. *Trans. Faraday Soc.* **1945**, *41*, 333.
(72) Llopis, J.; Sancho, A. Electrochemical Corrosion of Platinum in Hydrochloric Acid Solutions. *J. Electrochem. Soc.* **1961**, *108*, 720.
(73) Kuhn, A. T.; Wright, P. M. A Study of the Passivation of Bright Platinum Electrodes During Chlorine Evolution from Concentrated Sodium Chloride Solutions. *J. Electroanal. Chem. Interfacial Electrochem.* **1972**, *38*, 291.

(74) Chambers, J. F.; Stokes, J. M.; Stokes, R. H. Conductances of Concentrated Aqueous Sodium and Potassium Chloride Solutions at 25 °C. *J. Phys. Chem.* **1956**, *60*, 985.

(75) Newman, J. Resistance for Flow of Current to a Disk. *J. Electrochem. Soc.* **1966**, *113*, 501.

(76) Levich, V. G. *Physicochemical Hydrodynamics*; Prentice-Hall: Englewood Cliffs, NJ, 1962.

(77) Schmiedl, R.; Demuth, V.; Lahnor, P.; Godehardt, H.; Bodschwinna, Y.; Harder, C.; Hammer, L.; Strunk, H. P.; Schulz, M.; Heinz, K. Oxygen Diffusion Through thin Pt Films on Si(100). *Appl. Phys. A: Mater. Sci. Process.* **1996**, *62*, 223.